



**HAL**  
open science

## Passive monitoring of nonlinear relaxation of cracked polymer concrete samples using Acoustic Emission

Xiaoyang Yu, Mourad Bentahar, Charfeddine Mechri, Silvio Montrésor

### ► To cite this version:

Xiaoyang Yu, Mourad Bentahar, Charfeddine Mechri, Silvio Montrésor. Passive monitoring of nonlinear relaxation of cracked polymer concrete samples using Acoustic Emission. *Journal of the Acoustical Society of America*, 2019, 10.1121/1.5127519 . hal-02462731

**HAL Id: hal-02462731**

**<https://univ-lemans.hal.science/hal-02462731v1>**

Submitted on 31 Jan 2020

**HAL** is a multi-disciplinary open access archive for the deposit and dissemination of scientific research documents, whether they are published or not. The documents may come from teaching and research institutions in France or abroad, or from public or private research centers.

L'archive ouverte pluridisciplinaire **HAL**, est destinée au dépôt et à la diffusion de documents scientifiques de niveau recherche, publiés ou non, émanant des établissements d'enseignement et de recherche français ou étrangers, des laboratoires publics ou privés.

## Passive monitoring of nonlinear relaxation of cracked polymer concrete samples using acoustic emission

Xiaoyang Yu, Mourad Bentahar, Charfeddine Mechri, and Silvio Montrésor

Citation: *The Journal of the Acoustical Society of America* **146**, EL323 (2019); doi: 10.1121/1.5127519

View online: <https://doi.org/10.1121/1.5127519>

View Table of Contents: <https://asa.scitation.org/toc/jas/146/4>

Published by the *Acoustical Society of America*

---

### ARTICLES YOU MAY BE INTERESTED IN

[Deep transfer learning for source ranging: Deep-sea experiment results](#)

*The Journal of the Acoustical Society of America* **146**, EL317 (2019); <https://doi.org/10.1121/1.5126923>

[Analysis of spherical isotropic noise fields with an A-Format tetrahedral microphone](#)

*The Journal of the Acoustical Society of America* **146**, EL329 (2019); <https://doi.org/10.1121/1.5127736>

[Broadband sound propagation in a seagrass meadow throughout a diurnal cycle](#)

*The Journal of the Acoustical Society of America* **146**, EL335 (2019); <https://doi.org/10.1121/1.5127737>

[A tutorial example of duct acoustics mode detections with machine-learning-based compressive sensing](#)

*The Journal of the Acoustical Society of America* **146**, EL342 (2019); <https://doi.org/10.1121/1.5128399>

[Calculation of acoustic radiation modes by using spherical waves and generalized singular value decomposition](#)

*The Journal of the Acoustical Society of America* **146**, EL347 (2019); <https://doi.org/10.1121/1.5128139>

[Three-dimensional acoustic propagation effects induced by the sea ice canopy](#)

*The Journal of the Acoustical Society of America* **146**, EL364 (2019); <https://doi.org/10.1121/1.5129554>

---



**JASA**  
THE JOURNAL OF THE  
ACOUSTICAL SOCIETY OF AMERICA

**Special Issue:**  
**Additive Manufacturing and Acoustics**

Submit Today!



# Passive monitoring of nonlinear relaxation of cracked polymer concrete samples using acoustic emission

Xiaoyang Yu, Mourad Bentahar,<sup>a)</sup> Charfeddine Mechri,<sup>b)</sup>  
and Silvio Montrésor

*Laboratoire d'Acoustique de l'Université du Mans, UMR-CNRS 6613, Le Mans Université,  
Av. Olivier Messiaen, 72085 Le Mans Cedex 9, France  
xiaoyang.yu@univ-lemans.fr, mourad.bentahar@univ-lemans.fr,  
cherfeddine.mechri@univ-lemans.fr, silvio.montrésor@univ-lemans.fr*

**Abstract:** This work presents an acoustic emission (AE) monitoring of slow dynamics in micro-cracked polymer concrete (PC) samples. In order to obtain calibrated damage states, AE was first used to characterize the micro-damage mechanisms in real time when PC samples are submitted to three-point bending tests. Then, an unsupervised classification of AE data based on the Principle Component Analysis and the *k*-means clustering was applied to classify AE data. The AE monitoring of the nonlinear relaxation of PC samples revealed the existence of a silence period followed by AE hits belonging to two different damage classes. A similarity appeared between the properties of the detected AE hits obtained during the nonlinear relaxation and the quasi-static tests. Finally, this work shows that the dynamics of both mechanisms during the nonlinear relaxation are clearly different.

© 2019 Acoustical Society of America

[CCC]

Date Received: July 8, 2019 Date Accepted: September 2, 2019

## 1. Introduction

Consolidated granular media are known to be nonlinear hysteretic even at the initial intact state.<sup>1,2</sup> Due to the existing features at their microscopic scale (micro-cracks, interfaces, etc.), these materials manifest a hysteretic stress-strain relationship when excited with an ultrasonic wave.<sup>3</sup> Depending on the time scale, two kinds of observations can be performed on such materials. First, the fast-dynamic, which appears quite instantaneously, can be observed by tracking either the generated higher order harmonics,<sup>4</sup> the shift of the resonance frequency,<sup>5</sup> or the non-application of the superposition principle,<sup>6</sup> etc., as a function of the excitation amplitude. Besides the instantaneous effect, the excitation amplitude brings the material into a new elastic state by slowly changing damping and elastic modulus during a period of time which can take minutes. Therefore, the new values of damping and elastic modulus will not change again as long as the excitation amplitude is maintained constant. Once the excitation is removed, the material properties recover slowly their initial values until the original equilibrium state is reached.<sup>5,7</sup> In general, the observation of slow dynamics is performed in two steps. The material is first conditioned (softened) when excited at dynamic strains corresponding to  $\sim 10^{-6}$  or higher. When the full conditioning is reached, the material is excited at a very weak strain (depending on the experimental conditions such as the signal-to-noise ratio) in order to probe relaxation. The latter evolves as the logarithm of time over minutes, hours, or days depending on the conditioning characteristics. In a previous work,<sup>8</sup> the existing link between the evolution of slow dynamics (i.e., relaxation time) and acoustic emission (AE) (i.e., energy) recorded during the gradual damaging of composites was proved. However, the AE hits were not recorded during the relaxation of the composites but only during the creation of cracks. In order to better understand the slow dynamic phenomenon, this letter presents new experimental results which emerge from the monitoring of relaxation using AE as a passive monitoring tool in the absence of the usually used weak excitation. Furthermore, this work shows the existence of a resemblance between AE hits recorded during the creation of cracks and the ones emitted during the relaxation of the polymer concrete (PC).

<sup>a)</sup> Author to whom correspondence should be addressed.

<sup>b)</sup> Also at: CTTM, 20 Rue Thalès de Milet, Le Mans, France.

## 2. AE during quasi-static tests

This study is conducted on PC specimens ( $200 \times 40 \times 40 \text{ mm}^3$ ), manufactured simultaneously at the same conditions and made of epoxy resin, sand, and gravel at 40%, 30%, and 30% volume fractions, respectively. An Instron<sup>TM</sup> universal testing machine with a 10 kN capacity and 0.05 mm/min crosshead velocity was used to test specimens up to their final rupture using a three-point bending. Once the average maximum charge is determined, intermediate damage levels were created. During the different mechanical tests, the creation and propagation of micro-cracks were monitored using AE sensors in order to detect the transient elastic waves emitted by the created cracks. This was performed using MISTRAS<sup>TM</sup> system and two piezoelectric sensors ( $WS_x$ ) with a frequency bandwidth [100 kHz–1 MHz]. AE hits were pre-amplified at 40 dB, bandpass filtered (20 kHz–1 MHz) and sampled using a PCI card at a sampling rate of 5 MHz [Fig. 1(a)]. AE hits were separated in time using the following time filters: Peak Definition Time (50  $\mu\text{s}$ ), Hit Definition Time (100  $\mu\text{s}$ ), and Hit Lock Time (400  $\mu\text{s}$ ). Finally, the detection threshold was set at 40 dB, where 0 dB corresponds to 1  $\mu\text{V}$ .

In Fig. 1(b) the increase of the AE activity as a function of the applied load can be clearly seen, and suggests an amplitude-based classification of AE signals. Indeed, during the damaging of the PC, various types of micro-cracks can be created within the different constituents (resin matrix, resin/gravel or resin/sand interface, gravel) depending on the experimental conditions. However, the acoustic signature of a given damage mechanism not only depends on amplitude, but also depends on time and/or frequency domain parameters contained within the AE hits. In this study, we used an unsupervised classification of AE data based on the Principle Component Analysis and the  $k$ -means clustering. For the considered nine AE hit features (amplitude, duration, rise time, counts, counts to peak, energy, peak frequency, frequency centroid, and weighted frequency), four principal components were injected as inputs of the  $k$ -means. The optimal clustering is determined according to the minimum values of Davies–Bouldin index ( $R_{DB}$ ) for clustering validation,

$$R_{DB} = \frac{1}{k} \sum_{i=1}^{i=k} \max_{i \neq j} \left( \frac{d_i + d_j}{d_{ij}} \right), \quad (1)$$

where  $k$  is the number of selected classes,  $d_i$  and  $d_j$  are the average distances in the  $i$ th and  $j$ th class, and  $d_{ij}$  is the average distance between classes  $i$  and  $j$ . Results show that the minimum  $R_{DB}$  is obtained for  $k=3$ , which means that signals can be separated into three classes as shown in Fig. 2. Two classes (CL<sub>1</sub> and CL<sub>2</sub>) appear almost simultaneously from the beginning of the mechanical test, whereas the third class CL<sub>3</sub> appears during a more advanced state of damage. It is interesting to note that CL<sub>1</sub> signals have low amplitudes and low frequency components, whereas CL<sub>2</sub> signals have higher amplitudes and contain greater frequency components. Based on bending tests performed on pure resin samples, gravel-resin and sand-resin samples, and results from the literature,<sup>9</sup> CL<sub>1</sub> and CL<sub>2</sub> signals refer to matrix micro-cracking, and sand-matrix debonding, respectively. CL<sub>3</sub> signals were also found in the gravel-resin samples. Experiments show that they refer to a gravel-matrix debonding mechanism and their energy is the most important one found during the PC damaging. Finally, we note that in view of the big difference existing between the elastic moduli of the PC constituents associated to the type of the mechanical test (bending), the micro-cracking of the gravel is not involved in the final rupture of the PC. This point was also verified

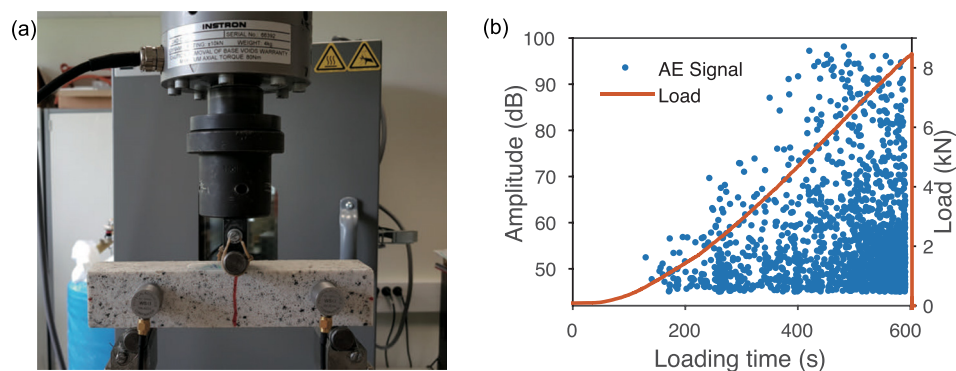


Fig. 1. (Color online) (a) PC sample submitted to a three-point bending test. (b) Evolution of the AE activity (amplitude of hits) during loading.

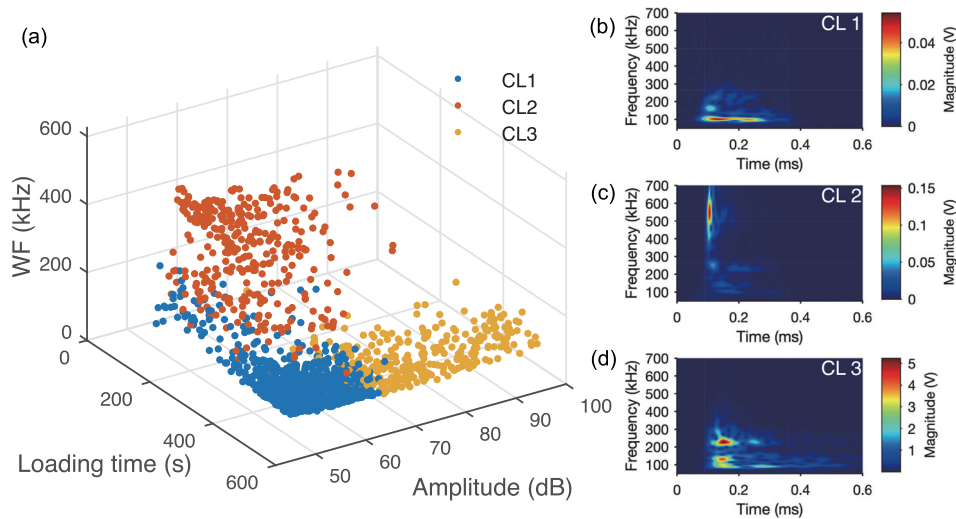


Fig. 2. (Color online) (a) Results of the unsupervised classification of AE hits (weighted frequency, amplitude, mechanical test duration). (b)–(d) Time frequency characteristics of the identified three damage classes.

through breaking facies observations performed after the final rupture of the different PC samples.

### 3. AE during dynamic tests

There is abundant literature on the use of AE as a tool to monitor the creation and propagation of micro-cracks when materials are submitted to quasi-static or dynamic stresses. However, once the cracks are already created, conventional ultrasonic methods (pitch-catch, thru transmission, etc.) are used instead. In the following, the AE is used on a partially damaged PC samples in order to detect the existing damage and monitor the relaxation during slow dynamics.

#### 3.1 Slow dynamics

Slow dynamic experiments were performed on partially damaged samples loaded up until  $\sim 50\%$  of their maximum charge. Samples were excited around their fundamental bending resonance using a swept-sine signal which lasts 40 s between 230 Hz and 250 Hz. A weak amplitude signal is first applied and the linear properties are probed at the intact and damaged states using ten consecutive swept-sine signals. The amplitude is then amplified ( $\times 200$ ) and PC samples are excited continuously until they reach the full conditioning state. Note that during conditioning, the viscoelastic properties are continuously changing until PC samples reach a new equilibrium state ( $\sim 300$  s of high amplitude excitation). At this time, the amplitude is set back to the same weak level (10 mV) in order to probe the PC relaxation during which the viscoelastic properties (e.g., the resonance frequency and damping) do not go back instantaneously to their original values, but follow a very slow recovery ( $\sim 90$  min). The log-time evolutions of resonance frequency and damping are presented in Fig. 3. This behavior, which is observed for different media (consolidated and unconsolidated granular, damaged metals or composites, etc.) is due to the hysteretic relationship existing between stress and strain where different microstructural features can be involved (sliding or frictional interfaces,<sup>10,11</sup> clapping micro-cracks,<sup>12</sup> etc.).

#### 3.2 Slow dynamics and AE

In order to probe the relaxation in the absence of the probe wave (10 mV), we propose the new protocol presented in Fig. 4(a). First, we verified the absence of any AE activity in intact PC samples at 0 V and 10 mV during  $\sim 2$  h. Then, we applied the same high drive signal (200 V) in order to reach the full conditioning state. The amplitude is then set back to zero in order to probe passively the relaxation of PC samples. Relaxation experiments were repeated on three damaged PC samples at successive days. The trends presented in this letter were reproducible within the range of  $\pm 15\%$  in terms of silence period, energy, cumulated energy, etc. At the intact state, and after the full conditioning, we did not detect any AE activity even when the AE detection threshold was considerably decreased (30 dB, where 0 dB refers to  $1 \mu\text{V}$ ). When the PC samples are damaged, we noticed the absence of AE activity during the first minutes of relaxation ( $\sim 500$  s depending on the considered PC sample). Following this period



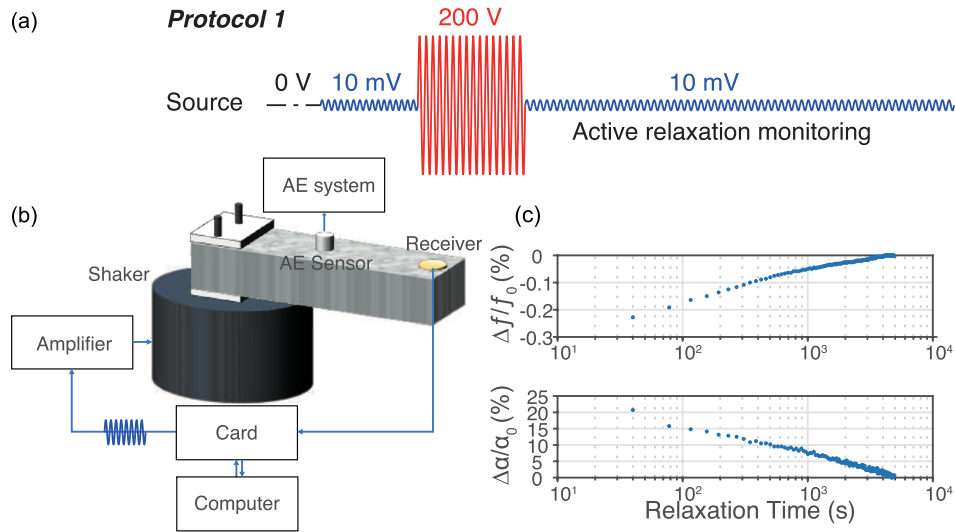


Fig. 3. (Color online) (a) Active relaxation monitoring protocol. (b) Experimental setup used to perform the nonlinear measurements with and without AE. (c) Log time-evolution of the relative resonance frequency ( $\Delta f/f_0$ ) and damping ( $\Delta\alpha/\alpha_0$ ) during relaxation. The linear properties of intact and damaged PC samples are ( $f_0^{\text{intact}} = 265.2 \text{ Hz}$ ,  $\alpha_0^{\text{intact}} = 7.3$ ) and ( $f_0^{\text{Damaged}} = 243.1 \text{ Hz}$ ,  $\alpha_0^{\text{Damaged}} = 6.7$ ), respectively.

of “silence,” we started to detect AE hits whose number was gradually increasing as a function of the relaxation time. Results show that the cumulative energy of the detected AE signals changes as the logarithm of relaxation time, and is therefore proportional to the evolution of  $\Delta f/f_0$  [presented in Fig. 3(c)] as can be seen in Fig. 4(b).

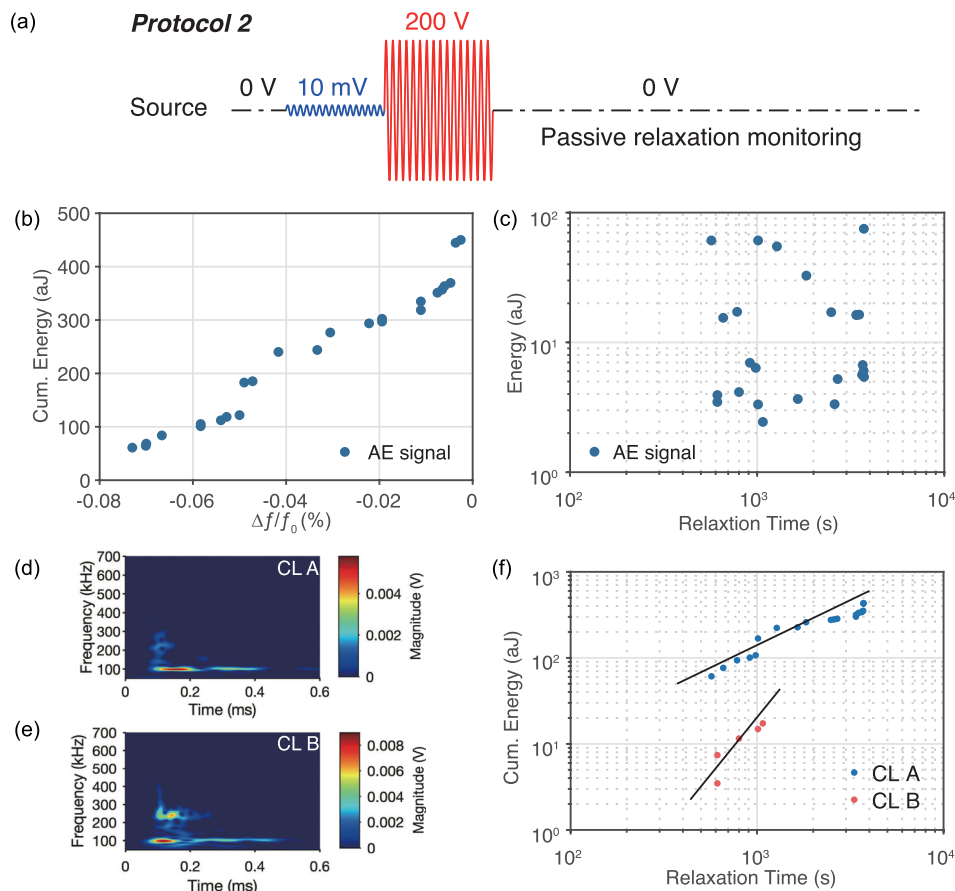


Fig. 4. (Color online) (a) Passive relaxation monitoring protocol. (b) Proportionality between cumulative energy of AE signals and resonance frequency determined during passive and active relaxation monitoring, respectively. (c) Energy of the detected AE signals detected during the relaxation of PC samples. (d) and (e) Time-frequency characteristics of (CL<sub>A</sub>) and (CL<sub>B</sub>) during relaxation. (f) Time evolution of the detected two damage classes (CL<sub>A</sub>) and (CL<sub>B</sub>) during the nonlinear relaxation of PC samples.

Table 1. Characteristics of AE signals (CL<sub>A</sub>) and (CL<sub>B</sub>) detected during the relaxation of damaged PC samples.

Class	Amplitude	Energy	RT	Duration	Counts		Peak	Center	WF
					Counts	to peak	Frequency	Frequency	
CL <sub>A</sub>	30–40 dB	5–80 aJ	30–50 $\mu$ s	200–400 $\mu$ s	30–60	10–20	100–120 kHz	100–150 kHz	100–120 kHz
CL <sub>B</sub>	30–33 dB	1–10 aJ	5–20 $\mu$ s	100–200 $\mu$ s	10–30	10–20	200–300 kHz	200–300 kHz	180–220 kHz

It is important to recall that in the proposed passive method the relaxation “stops” at the time when no AE is detected, even if the monitoring time is much longer than the above-mentioned 90 min (more than 2 h). In the active method (monitoring of resonance frequency and attenuation), the relaxation time is determined once the full recovery of the initial properties is reached. Results show that the relaxation time based on the passive approach coincides with  $\sim 97\%$  of frequency and damping recovery. The most likely hypothesis about the period of silence would be that the increase of damping due to conditioning prevents AE hits to reach the surface of the PC sample with sufficient amplitude. Indeed, with the help of attenuation results presented in Fig. 3(c), we can see that the silence period (which lasts  $\sim 500$  s) corresponds to a decrease, or recovery, of the relative damping ( $\Delta\alpha/\alpha_0$ ) from  $\sim 20\%$  to  $\sim 10\%$ . Figure 4(c) shows that the energy of the detected AE signals (i.e., the elastic energy released by the material) is becoming less important as a function of relaxation time. Note that this effect is in accordance with the evolution of the resonance frequency and damping since they both reach a limit value  $f_0$  and  $\alpha_0$  at the end of the relaxation. For this reason and for reasons related to the fact that the different ultrasonic paths are equivalent (localized damage), we did not perform attenuation compensation in this work.

Results show that amplitudes of the detected AE hits ( $\sim 5$  mV) during relaxation are significantly lower than those detected during the quasi-static bending loading (up to  $\sim 5$  V). The classification of the AE hits, based on the above-described clustering method, revealed the existence of two classes of AE signals, CL<sub>A</sub> and CL<sub>B</sub>, as can be seen in Table 1. Both types of signals are detected right after the silence period and CL<sub>A</sub> was the only one to be detected until the end of the PC relaxation. Furthermore, the properties of AE signals obtained during the passive relaxation measurements and those corresponding to damage mechanisms created during the quasi-static tests appeared to be similar. Indeed, the identified CL<sub>A</sub> and CL<sub>B</sub> classes strongly resemble the matrix cracking and gravel/matrix debonding, as it can be observed through the time-frequency signatures [Figs. 4(d) and 4(e)]. Also, we found that the dynamics of both mechanisms during relaxation are clearly different. Indeed, beyond the provided information to the overall measurement (i.e., carried out using a probe wave), AE shows that CL<sub>B</sub> relaxation is  $\sim 3$  times faster than the one of CL<sub>A</sub> [Fig. 4(b)]. This result shows that the use of AE as a tool to monitor slow dynamics helps to detect the most emissive (or energetic) events spontaneously operated within materials (in relation to the micro-mechanisms involved) and brings an experimental evidence for the follow-up of stress variation along the existing cracks for a better understanding of slow dynamics in complex media.

#### 4. Conclusion

This work has allowed going beyond the results previously found on sheet molding compound composite<sup>8</sup> by showing the capabilities of AE to passively monitor nonlinear relaxation of PC samples. The application of a new protocol associated to an appropriate signal processing on the same samples, before and after the creation of micro-cracks, shows that all damage mechanisms do not relax continuously and simultaneously as a function of time. The absence of AE signals in the case of intact PC samples is mainly due to the absence of micro-cracks, contrary to civil engineering concrete in which micro-cracks are normally created during the dry operation even at the intact state. Results obtained recently on civil engineering samples (not shown here) suggest that the presence of cracks is at the origin of the detected AE signals. Furthermore, results show that damage mechanisms do not relax with the same velocity and do not involve the same amount of energy. In our case, this suggests that the contribution of the micro-cracks created within the polymer matrix (CL<sub>A</sub>) represent the most involved mechanism during relaxation (and may be during conditioning). In order to complete the performed analysis, a comparison between AE signals involved during conditioning and relaxation is underway to include new consolidated granular materials such as civil engineering concrete.

**References and links**

- <sup>1</sup>R. A. Guyer and P. A. Johnson, *Nonlinear Mesoscopic Elasticity: The Complex Behaviour of Rocks, Soil, Concrete* (Wiley-VCH, Germany, 2009).
- <sup>2</sup>P. Antonaci, C. Bruno, P. Bocca, M. Scalerandi, and A. Gliozzi, “Nonlinear ultrasonic evaluation of load effects on discontinuities in concrete,” *Cement Concrete Res.* **40**(2), 340–346 (2010).
- <sup>3</sup>K. E. Claytor, J. R. Koby, and J. A. TenCate, “Limitations of Preisach theory: Elastic aftereffect, congruence, and end point memory,” *Geophys. Res. Lett.* **36**(6), L06304, <https://doi.org/10.1029/2008gl036978> (2009).
- <sup>4</sup>J. H. Cantrell and W. T. Yost, “Acoustic harmonic generation from fatigue-induced dislocation dipoles,” *Philos. Mag. A* **69**(2), 315–326 (1994).
- <sup>5</sup>M. Bentahar, H. E. Aqra, R. E. Guerjouma, M. Griffa, and M. Scalerandi, “Hysteretic elasticity in damaged concrete: Quantitative analysis of slow and fast dynamics,” *Phys. Rev. B* **73**(1), 014116 (2006).
- <sup>6</sup>M. Scalerandi, A. S. Gliozzi, C. L. E. Bruno, D. Masera, and P. Bocca, “A scaling method to enhance detection of a nonlinear elastic response,” *Appl. Phys. Lett.* **92**(10), 101912 (2008).
- <sup>7</sup>M. Scalerandi, A. S. Gliozzi, C. L. E. Bruno, and P. Antonaci, “Nonequilibrium and hysteresis in solids: Disentangling conditioning from nonlinear elasticity,” *Phys. Rev. B* **81**(10), 104114 (2010).
- <sup>8</sup>M. Bentahar and R. E. Guerjouma, “Monitoring progressive damage in polymer-based composite using nonlinear dynamics and acoustic emission,” *J. Acoust. Soc. Am.* **125**(1), EL39–EL44 (2009).
- <sup>9</sup>A. Marec, J. H. Thomas, R. E. Guerjouma, and R. Berbaoui, “Investigation of damage mechanisms of composite materials: Multivariable analysis based on temporal and wavelet features extracted from acoustic emission signals,” in *Springer Proceedings in Physics* (Springer, Berlin, Heidelberg, 2009), pp. 399–409.
- <sup>10</sup>E. Shalev, V. Lyakhovskiy, A. Ougier-Simonin, Y. Hamiel, and W. Zhu, “Inelastic compaction, dilation and hysteresis of sandstones under hydrostatic conditions,” *Geophys. J. Int.* **197**(2), 920–925 (2014).
- <sup>11</sup>S. Delrue, V. Aleshin, K. Truyaert, O. B. Matar, and K. V. D. Abeele, “Two dimensional modeling of elastic wave propagation in solids containing cracks with rough surfaces and friction—Part II: Numerical implementation,” *Ultrasonics* **82**, 19–30 (2018).
- <sup>12</sup>G. Shkerdin and C. Glorieux, “Nonlinear modulation of lamb modes by clapping delamination,” *J. Acoust. Soc. Am.* **124**(6), 3397–3409 (2008).